Time of flight emission spectroscopy of laser produced nickel plasma: Short-pulse and ultrafast excitations

N. Smijesh,[1] K. Chandrasekharan,[1] Jagdish C. Joshi,[2] and Reji Philip[2,a)]
[1]*Laser and Nonlinear Optics Laboratory, Department of Physics, National Institute of Technology Calicut, Calicut 673601, India*
[2]*Ultrafast and Nonlinear Optics Lab, Light and Matter Physics Group, Raman Research Institute, Bangalore 560080, India*

(Received 8 March 2014; accepted 18 June 2014; published online 1 July 2014)

We report the experimental investigation and comparison of the temporal features of short-pulse (7 ns) and ultrafast (100 fs) laser produced plasmas generated from a solid nickel target, expanding into a nitrogen background. When the ambient pressure is varied in a large range of 10^{-6} Torr to 10^{2} Torr, the plume intensity is found to increase rapidly as the pressure crosses 1 Torr. Time of flight (TOF) spectroscopy of emission from neutral nickel (Ni I) at 361.9 nm ($3d^9(^2D)\ 4p \rightarrow 3d^9(^2D)\ 4s$ transition) reveals two peaks (fast and slow species) in short-pulse excitation and a single peak in ultrafast excitation. The fast and slow peaks represent recombined neutrals and un-ionized neutrals, respectively. TOF emission from singly ionized nickel (Ni II) studied using the 428.5 nm ($3p^63d^8(^3P)\ 4s \rightarrow 3p^63d^9\ 4s$) transition shows only a single peak for either excitation. Velocities of the neutral and ionic species are determined from TOF measurements carried out at different positions (i.e., at distances of 2 mm and 4 mm, respectively, from the target surface) on the plume axis. Measured velocities indicate acceleration of neutrals and ions, which is caused by the Coulomb pull of the electrons enveloping the plume front in the case of ultrafast excitation. Both Coulomb pull and laser-plasma interaction contribute to the acceleration in the case of short-pulse excitation. These investigations provide new information on the pressure dependent temporal behavior of nickel plasmas produced by short-pulse and ultrafast laser pulses, which have potential uses in applications such as pulsed laser deposition and laser-induced nanoparticle generation. © *2014 AIP Publishing LLC*. [http://dx.doi.org/10.1063/1.4885760]

INTRODUCTION

Laser-produced plasma (LPP) is transient in nature and plasma parameters, which unfold rapidly in time, are crucially dependent on material properties and ambient gas pressure, in addition to laser parameters such as fluence, pulse width, wavelength, and irradiation spot size. Plasma diagnostics are essential for tailoring plasma properties for various applications. Different diagnostic techniques available for the characterization of LPP include optical emission spectroscopy (OES), laser-induced fluorescence, Langmuir probing, mass spectrometry, and photo-thermal beam deflection. Temporal evolution of the transient plasma can be recorded using fast detectors such as photomultiplier tubes (PMTs) and intensified charge coupled devices (ICCDs). These studies are essential for understanding and modeling various processes in fundamental plasma physics and plasma hydrodynamics.

The interaction of LPP with ambient gas leads to an expansion involving several physical processes such as thermalization, attenuation, diffusion, electron-ion recombination, and shock wave formation, which is a fairly complex phenomenon.[1] While plume expansion at lower pressures can be accurately described by a Monte Carlo simulation, this model is insufficient at moderate and high pressures.[2,3] At higher pressures, a blast wave model fits the experimental results well in the earlier stages of plasma expansion,[4] whereas a shock wave model predicts the plume length with reasonable accuracy.[5] A three dimensional combined model for plasma plume formation and its expansion is available, which benefits from the advantages of both microscopic and continuous descriptions.[6]

In the case of LPP generated by nanosecond (short-pulse) lasers, the generated plasma will interact with the trailing part of the relatively long laser pulse and absorb energy from it. On the other hand, in the case of LPP generated by femtosecond (ultrafast) lasers, the laser pulse is too short to interact with the plasma because the electron-ion collision time and heat conduction time are in the order of picoseconds.[7,8] This situation results in different expansion dynamics for ns LPP and fs LPP. For instance, Neogi *et al.*[9] has observed double peaks and even triple peaks (under certain favorable conditions) in the temporal evolution of ns LPP in carbon, which arise apparently from the compression wave reaching the plasma front from the compressed gas ahead of it. Time of flight (TOF) spectroscopy and imaging are powerful tools to characterize the expansion dynamics (in time and space) of atomic and ionic species found in LPP plumes. For example, ICCD measurements performed in a ns Aluminum LPP have shown the possibility of plume splitting at low pressures.[10] Even though material removal efficiency[11] and laser plasma dynamics leading to the production of nanoparticles[12] have been discussed in literature, a complete theoretical understanding of the expansion process is yet to be

a)Author to whom correspondence should be addressed. Electronic mail: reji@rri.res.in

achieved. However, it has been shown that at relatively lower laser fluences, femtosecond laser produced plasmas consist of two different components, viz. atomic species and nanoparticles, in the earlier ($\sim$ 200 ns to 500 ns) and later ($\sim$ 100 μs) stages of plasma expansion, respectively. The fast atomic species can be observed once the fluence of the irradiating laser is increased well beyond the ablation threshold. Nanoparticle production can be maximized by optimizing the laser fluence.[13] Furthermore, it is reported that ultrafast ablation of high-Z materials can lead to higher nanoparticle yield when compared to low-Z materials.[14] It is reported that ultrafast laser ablation is one of the ways to produce nanoparticles of any material independent of the specific material properties, as the timescales involving ultrafast laser heating and material relaxation process are in the order of picoseconds.

In the present work, we have used short-pulse (7 ns) as well as ultrafast (100 fs) laser pulses to generate and characterize LPPs from a pure solid nickel target kept in nitrogen atmosphere, and have compared TOF spectra of the neutral and ionic species in the optical spectral region. Emission at 361.9 nm from the neutral Ni I species and that at 428.5 nm from the singly ionized Ni II species are studied in detail for ambient gas pressures in the range of 10^{-6} Torr to 10^{2} Torr. Emission intensity is found to depend on the background pressure and laser pulse width. From TOF measurements carried out at different axial points on the plasma plume, the occurrence of fast as well as slow neutrals, and fast ions, has been identified. Velocities of the species have been calculated, from which it is shown that the observed fast neutrals are formed from the recombination of fast ions and free electrons present in the plasma.

EXPERIMENTAL

We used 100 fs (FWHM) pulses at 800 nm from a regeneratively amplified Ti: sapphire laser (*TSA-10*, Positive Light) with a maximum energy of $\sim$10 mJ, and 7 ns pulses at 1064 nm from a Q-Switched Nd: YAG laser (*Quanta Ray*, Spectra Physics) with a maximum energy of $\sim$150 mJ, for irradiating the target. In both cases, the energies were adjusted such that the laser fluence was the same ($\sim$16 Jcm^{-2}) on the target surface, which is well above the ablation threshold. The nickel sample used (ACI Alloys, Inc., San Jose) has purity better than 99.99%. Even though the lasers are set to run at 10 Hz for energy stability, the measurements are taken in the single-shot mode. In the case of the ns laser, this was achieved by triggering the Q-switch externally, while for the fs laser, a fast mechanical shutter was employed in the beam path. An electronic synchronization circuit drives the shutter so that single pulses can be selected at will from the 10 Hz pulse train. In order to avoid target pitting, after each laser pulse, the sample was moved by about 0.5 mm using a stepper motor driven X-Y translator, so that the next laser pulse falls on a fresh point on the target surface.

Optical emission and TOF spectra were measured by means of a monochromator (*iHR320*, Horiba Jobin Yvon) equipped with a CCD detector (*Synapse*, Horiba Jobin Yvon) and PMT (*R943–02*, Hamamatsu). Plasma emission was collected and focused to the monochromator using two lenses and a mirror, which were fixed on a high resolution translation stage. By moving the stage, emission from any part of the plume could be recorded (Figure 1). Emission lines in the spectra recorded at a resolution of 0.06 nm were assigned by comparison with the standard NIST atomic spectral database.[15] The TOF spectra of neutral Ni I line at 361.9 nm and ionic Ni II line at 428.5 nm measured for various ambient pressures using the PMT were recorded on a fast digital storage oscilloscope (*DPO 7354*, Tektronix).

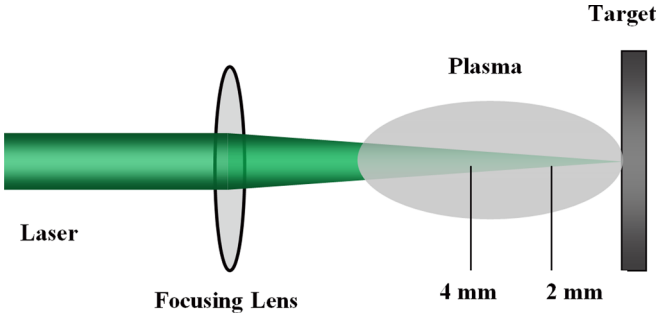

FIG. 1. Geometry of the LPP experiment. Focused laser pulses irradiate a solid nickel target to form an expanding plasma plume. Most of the spectral measurements were made at distances of 2 mm and 4 mm from the target surface.

OPTICAL EMISSION SPECTROSCOPY

OES is a powerful non-destructive technique for plasma characterization.[16] We studied emission from the excited state of neutral nickel (Ni I) at the wavelengths of 356.6 nm, 361.9 nm, 377.5 nm, 378.3 nm, 380.6 nm, and 385.9 nm, and that from the singly ionized state of nickel (Ni II) at 428.5 nm. Intensity at these wavelengths as a function of ambient pressure, measured 2 mm away from the target surface, is shown in Figures 2(a) and 2(b) for ns LPP and fs LPP, respectively. A sharp increase in the intensity is found around 1 Torr in both cases. In general, at low ambient pressures, the plume expands more, reducing the number density and collisions, and therefore, the ionization rate. At high pressures, the plume is smaller and the collision rate increases leading to an enhanced ionization; however, the mass of ablated material reduces due to laser-plasma coupling in ns LPP,[17] and filamentation may lead to ineffective laser-target coupling at very high ambient pressures in fs LPP.[18] Even though we do not see any reduction in plume intensity up to an ambient pressure of 10^{2} Torr, the above effects might reduce plume intensity at still higher pressures.

TIME OF FLIGHT SPECTROSCOPY

In pulsed laser ablation, the energy absorbed from the laser pulse is utilized for processes such as heat conduction, melting, and vaporization of the material surface. Target will be ablated if the light intensity is above the ablation threshold, and the ablated species will interact with the surrounding gas.[1,9] The ablation threshold I_{min}, which is defined as the minimum power density required for vaporizing the material, is given by

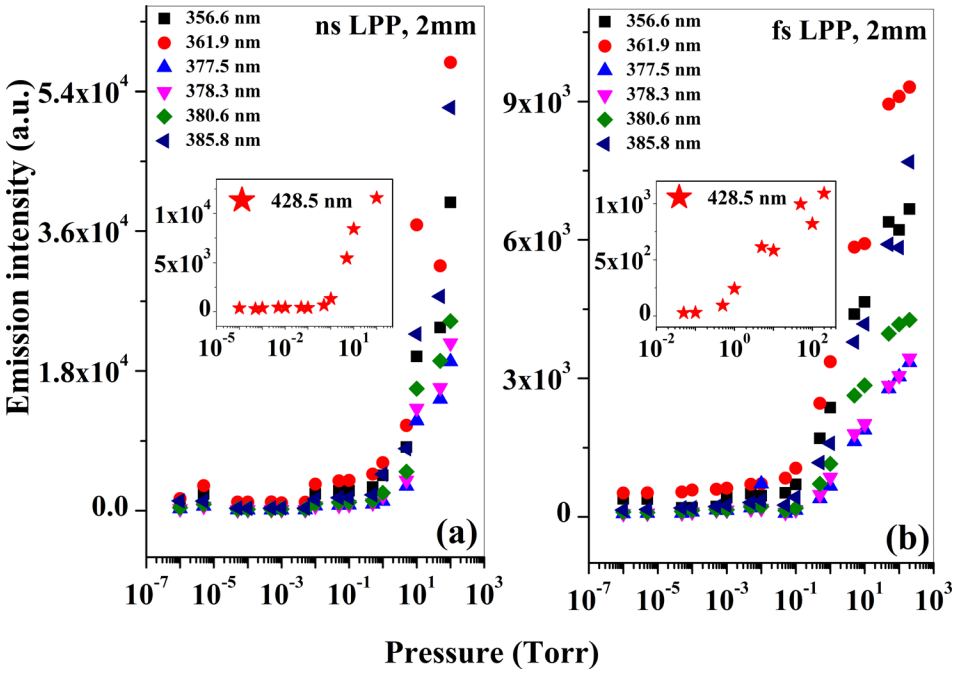

FIG. 2. Integrated emission intensity of the Ni I spectral lines measured at a distance of 2 mm from the target surface, for (a) 7 ns and (b) 100 fs irradiation. Insets show the 428.5 nm line emitted by the Ni II species. Intensity rises sharply around an ambient pressure of 1 Torr. ns LPP is more intense compared to fs LPP.

$$I_{min} = \frac{\rho L_v k^{\frac{1}{2}}}{\Delta t^{1/2}} \quad (1)$$

where ρ is the density of the material, L_v is the latent heat of vaporization, k is the thermal diffusivity, and Δt is the laser pulse width. I_{min} is calculated to be 8.69×10^{11} W/cm^2 for fs excitation and 3.89×10^{8} W/cm^2 for ns excitation in the present case, with the corresponding laser fluences being 8.69×10^{-2} J/cm^2 and 1.94 J/cm^2, respectively. However, since the applied fluence is high at 16 J/cm^2, and electron-ion collisions and heat conduction occur in the order of picoseconds, material ablation will happen rapidly by the leading edge of the laser pulse itself for ns excitation. Ablation creates a high density region near the target called the Knudsen layer, which shields the rest of the pulse from reaching the target surface.[12] Therefore, the evaporated material will absorb energy from the trailing edge of the ns pulse. On the other hand, the whole energy associated with the pulse will be directly deposited on the target surface in fs LPP, since the laser pulse is too short for any laser-plasma interaction to occur. Therefore, the dynamics of plume formation and its expansion to the surroundings are entirely different between short-pulse and ultrafast excitations.[9,10]

We performed time of flight emission measurements on the bound-bound transition $3d^9(^2\mathrm{D})\ 4p \rightarrow 3d^9(^2\mathrm{D})\ 4s$ occurring at 361.9 nm (Ni I) to understand the propagation of Ni neutrals through the expanding plasma. Measurements were taken for the 2 mm and 4 mm axial positions in the plume along the expansion direction. Figures 3(a) and 3(b) show the TOF spectra observed at 2 mm for ns LPP in the studied pressure range. The temporal profile of Fig. 3(a) shows a double-peak structure (fast peak P1 and slow peak P2), which corresponds to fast and slow neutrals appearing at different times ($\sim$ 80 ns and 210 ns, respectively) in the expanding plume. Emission intensity from fast neutrals (with narrow TOF width) is found to be low compared to that from slow neutrals (with relatively broader TOF signature) in the pressure range of 10^{-7} to 10^{-2} Torr (Fig. 3(a)). On the other hand, in the range of 10^{-2} to 5 Torr, emission intensity from fast neutrals substantially builds up (Fig. 3(b)). This observation indicates that P1 can be attributed to the emission from neutral nickel formed by the recombination of fast ionic species with free electrons (which is independently corroborated from ion TOF measurements as discussed later), while P2 corresponds to the comparatively slower un-ionized neutral atoms present in the ablated material.[11] Collisions among

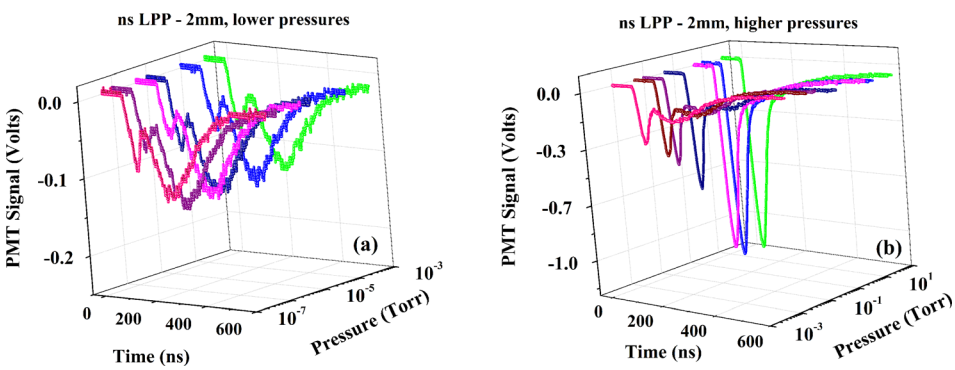

FIG. 3. Time of flight emission spectra of the 361.9 nm ($3d^9(^2\mathrm{D})\ 4p \rightarrow 3d^9(^2\mathrm{D})\ 4s$) transition from Ni I, measured in the plasma plume at a distance of 2 mm from the target surface, for 7 ns irradiation. Ambient pressure varies from (a) 10^{-7} to 10^{-3} Torr and (b) 10^{-3} to 10^{2} Torr.

plasma species as well as heating of the plasma by absorption of energy from the trailing part of the laser pulse are more efficient at higher pressures, leading to enhanced ionization. This results in a higher recombination rate, leading to the enhancement of P1. For pressures $\geq$ 5 Torr, the two peaks combine to form a single broader peak with larger emission intensity, the arrival time of which is comparable to that of P1. This merging may be due to a concomitant reduction in the intensity of P2, which can be expected at high pressures due to plume confinement and thermal leak. Thermal leak from the plume is proportional to the density of background gas,[19] and is given by

$$Q_{\Delta t} = \frac{2m_e}{M_B}\,\sigma_{ea} n_B \left[\frac{5kT_e}{\pi m_e}\right]^{1/2}, \tag{2}$$

where n_B and M_B are the density and mass of the background gas, respectively, and σ_{ea} is the elastic scattering cross section of the electrons.

For ns irradiation, it is known that plasma temperature and electron density get enhanced with pressure.[20] The temperature increases due to plasma heating via confinement and enhanced laser-plasma coupling. The emitted species will interact with the trailing part of the laser pulse and absorb energy via inverse bremsstrahlung (IB), given by

$$\alpha_{IB} = 1.37 \times 10^{-35}\,\lambda^3 N_e^2 T_e^{-\frac{1}{2}}, \tag{3}$$

where α_{IB}, λ, and N_e (cm^{-3}) are the IB co-efficient, irradiation wavelength, and electron number density, respectively. This will cause a rise in the electron temperature, which results in further ionization as well as excitation through collisions with exited and ground state neutrals. Enhancement of IB is possible with increase in number density, and shielding and confinement will generate hotter plasma.[21] Thermal velocity of the plasma species will increase with temperature, and is proportional to $T_i^{1/2}$ for ions, given by

$$V_{T_i} = \left(\frac{ZKT_i}{m_i}\right)^{1/2}, \tag{4}$$

where V_{T_i}, Z, T_i, and m_i are the thermal velocity, ionization stage, temperature, and mass of the ion, respectively. The velocity is maximized in the core of the plasma, and reduces thereafter along the expansion direction via rapid cooling due to plasma-background interaction. This results in the species moving with lower velocities at larger distances from the target surface. Moreover, plasma temperature and number density will fall beyond certain optimum high pressures due to energy loss by collisions with background gas.

Figures 4(a) and 4(b) show the measured velocities of the fast and slow neutral species in the expanding ns plasma (velocity is calculated by dividing the distance of the measuring position from the target surface by the arrival delay of the TOF peak with respect to the laser pulse). As the ns plasma plume expands velocities of the fast and slow neutrals (P1 and P2, respectively) also change accordingly. For instance, P1 speeds up from ~30 km/s at 2 mm to ~70 km/s at 4 mm (Figure 4(a)). Moreover, while P1 velocity increases overall with pressure at 2 mm, it decreases with pressure at 4 mm. A local decrease in velocity can be seen for 2 mm in the pressure range of 10^{-4} to 10^{-2} Torr. Such a fluctuation in velocity can arise if a shock wave propagates back and forth through the ambient gas subsequent to ablation:[22] with a laser fluence of ~16 J/cm^2, ablation of the target is intense and rapid. In the case of P2 (Figure 4(b)), the velocity is much lower, and speeding from 2 mm to 4 mm is quite limited, showing, in fact, a deceleration at the higher pressures.

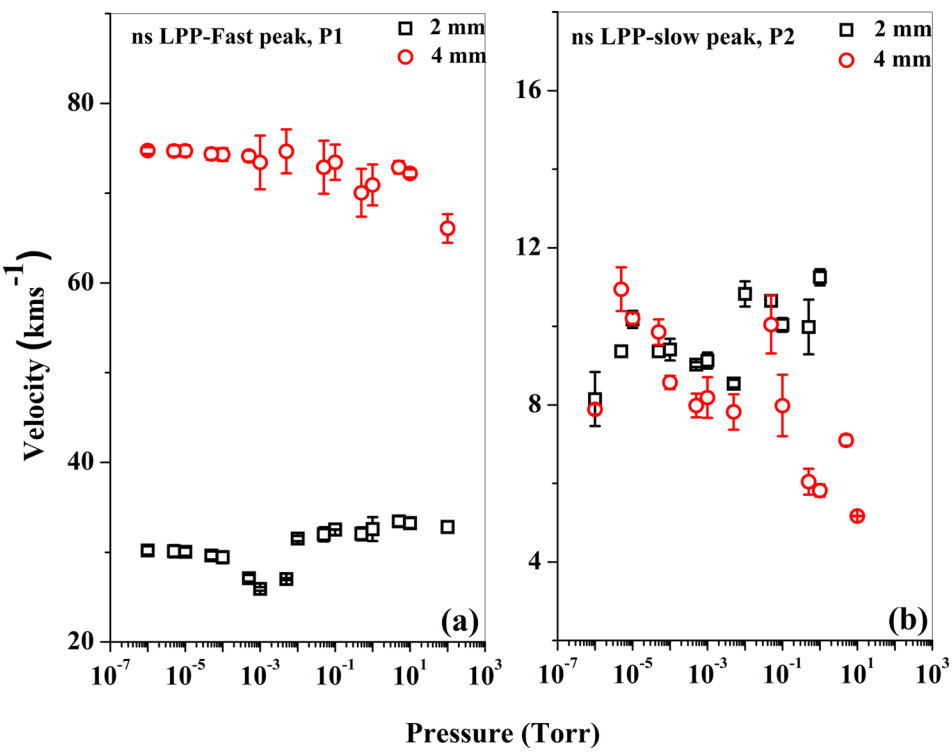

FIG. 4. Velocities of the (a) fast and (b) slow Ni I species, measured at axial distances of 2 mm and 4 mm from the target surface, for 7 ns irradiation.

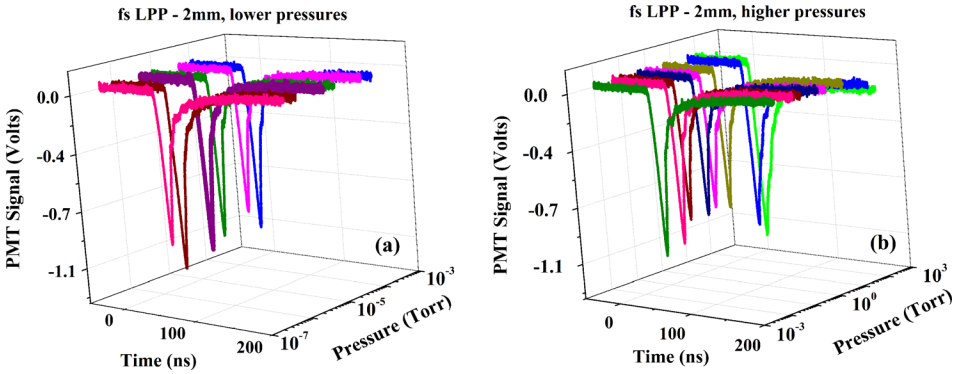

FIG. 5. Time of flight emission spectra of the 361.9 nm ($3d^9(^2D)\ 4p \rightarrow 3d^9(^2D)\ 4s$) transition of Ni I, measured in the plasma plume at a distance of 2 mm from the target surface, with 100 fs irradiation. Ambient pressure varies from (a) 10^{-7} to 10^{-3} Torr and (b) 10^{-3} to 10^{2} Torr.

While the pressure-dependent velocity increases at 2 mm may be attributed to laser-plasma interaction, the velocity decreases at 4 mm can be due to the confinement and fast cooling of the plasma.

Figures 5(a) and 5(b) depict TOF emission spectra of Ni I species from fs excitation, measured at the 2 mm position. Unlike ns LPP, fs LPP apparently shows only a single peak in the emission profile for all pressures studied, which arrives around 35 ns. The observed sharp leading edge could be due to the recombined species, and the trailing edge due to unionized species, which quickly follow one another. In addition, the emission lifetime is obviously shorter compared to that of ns excitation. The neutrals accelerate between the 2 mm and 4 mm positions, but the velocities are almost constant with respect to the ambient pressure (Figure 6). Absolute velocities are higher compared to the fast neutrals of ns LPP, but acceleration between the 2 mm and 4 mm positions is somewhat lower than that seen for ns excitation. While the acceleration seen for fs LPP is due exclusively to the Coulomb pull experienced by ions from the fast electrons moving ahead of them that seen in ns LPP should arise from both laser-plasma interaction and Coulomb pull. Essentially, the plasma front will expand with an acoustic velocity and accelerate to a certain distance before getting decelerated.[23] As mentioned before, the reasons for this acceleration are (i) Coulomb pull on the ions by the lighter electron cloud moving ahead, and repulsion caused by the field of ions near the emitting species, and (ii) thermal velocity acquired by the species due to plasma heating via collisions and photoionization, which is dependent on the nature and pressure of the background gas and pulse width of the irradiating laser.

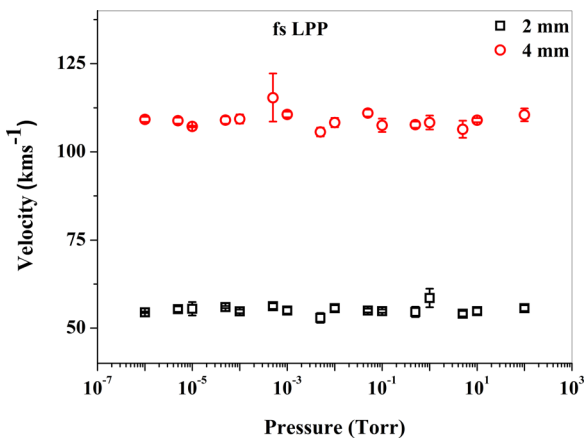

FIG. 6. Velocities of the Ni I species measured at axial distances of 2 mm and 4 mm from the target surface, for 100 fs irradiation.

In fs ablation, the entire energy of the laser pulse is dumped straight onto the target so that heating of the generated plasma by the trailing edge of the laser pulse is absent. The much higher intensity of the fs pulse generates a spontaneous magnetic field near the target surface, which pinches the expansion causing the plume to be confined along the axial direction.[24,25] This confinement enhances the number density of the fs plasma, compared to ns LPP generated under similar fluence conditions. The enhanced number density results in a higher acceleration of the emitters. These highly accelerated ions will recombine with free electrons to produce recombined neutrals, which arrive in the TOF faster than their ns LPP counterparts. This large acceleration, which, in fact, occurs without any laser-plasma interaction, can be clearly seen in Figure 6. Background pressure does not seem to affect the velocity up to a distance of 4 mm, though it might get affected at larger distances. The unionized neutrals from fs excitation might perhaps be separated in time if measured at longer distances, but it also requires that the TOF signals are strong enough for measurement at those distances.

Figures 7(a) and 7(b) show the TOF emission spectra of the singly ionized Ni II ions. Emission intensity is relatively lower compared to that of neutrals (see Figure 2). Emission from ions is less prominent because ion density is reduced at high pressures due to larger recombination rates, and at low pressures due to reduced collisions. Therefore, in the present experiments, emission from ionic species could be observed only for certain intermediate pressures. For ns LPP, emission could be measured from 0.05 Torr to 100 Torr but, for fs LPP, it could be measured only from 10 Torr to 100 Torr. Emission intensity increases as a function of pressure and peaks around 10 Torr for ns excitation. The peaking pressure could not be determined for fs excitation due to the limited range available for investigation.

Figures 8(a) and 8(b) depict the velocity of ionic species measured at 2 and 4 mm distances, for ns and fs ablations, respectively. For ns irradiation, velocity is almost a constant around 90 km/s at 2 mm irrespective of background pressure. Moreover, acceleration is not high at the lower pressures. This result supports the fact that fast neutrals are formed from the recombination of fast ions with free electrons. The lighter electrons will travel faster than the ions, and the

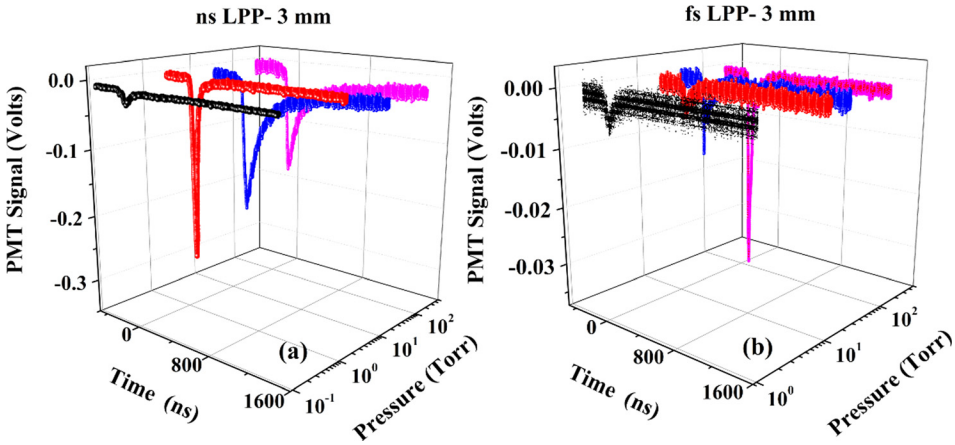

FIG. 7. Time of flight emission spectra of the 428.5 nm ($3p^6 3d^8 (^3P)\ 4s \rightarrow 3p^6 3d^9\ 4s$) transition of Ni II measured in the plasma plume at a distance of 3 mm from the target surface, for (a) 7 ns and (b) 100 fs irradiations.

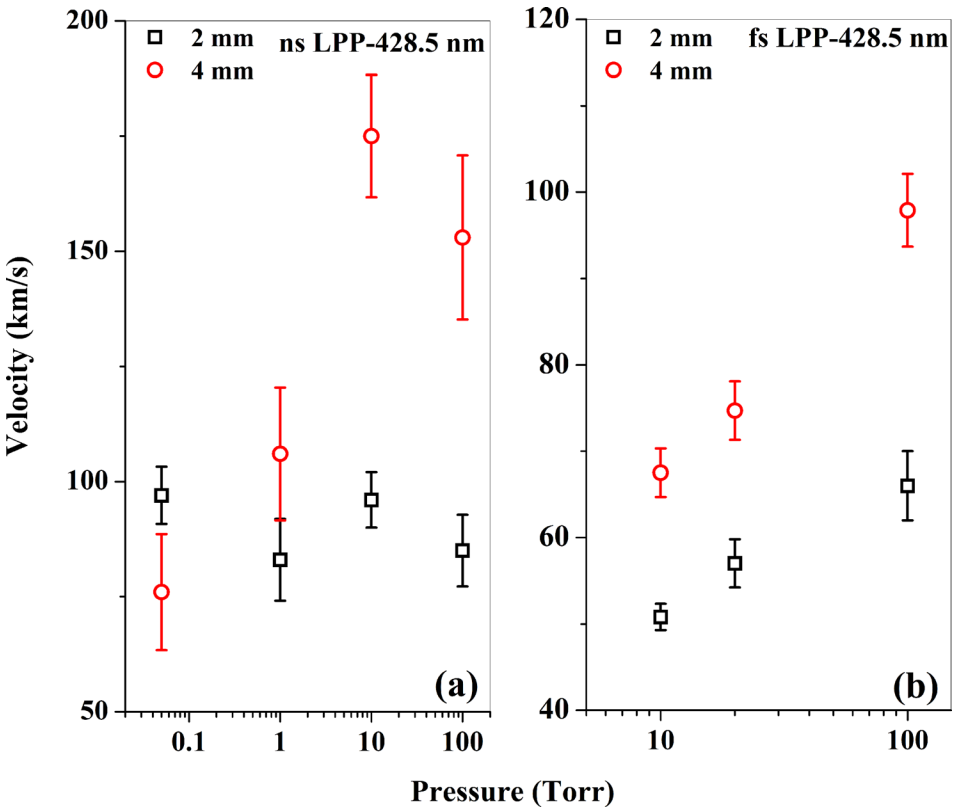

FIG. 8. Velocity of the Ni II species measured at axial distances of 2 mm and 4 mm from the target surface, for (a) 7 ns and (b) 100 fs irradiations.

Coulomb pull on the ions will be inversely proportional to the electron-ion distance. Thus, only those ions, which are quite fast, can recombine with the electrons. Assuming that most of the fast ions undergo recombination, only the slower ions (which also experience less Coulomb pull) will predominantly remain for detection. The acceleration will be smaller for these ions compared to those which went ahead of them. However, as we see from the figure acceleration can increase at higher pressures, where laser-plasma interaction is stronger: at the 4 mm position, velocity increases with pressure and reaches a maximum of 175 km/s. On the other hand, for fs irradiation, velocity increases linearly with pressure at both the 2 mm and 4 mm positions. Acceleration is higher for ns LPP due to the higher plume heating, and it is maximized around a certain pressure range[20,26] of 10 Torr in our case, where the emission peak intensity from ionic species also is a maximum. For our experiment, the right balance between collisions and recombinations is reached at this pressure to result in maximum ionization, and hence maximum Coulomb pull.

Our detailed studies reveal that for the 2 mm position, arrival times of the fast neutral species (33 ns to 70 ns) are similar to the arrival times of the ionized species (23 ns to 40 ns), whereas the arrival of the slow species takes place between 180 ns and 240 ns. This observation further affirms that the generation of fast atomic species in the expanding plume is indeed due to the recombination of fast ions with electrons. Detailed studies of the acceleration of neutrals in the LPP are underway to obtain more insights into the physical phenomena involved in this process.

CONCLUSION

In conclusion, we have generated and investigated laser produced nickel plasmas using short-pulse (7 ns) and ultrafast (100 fs) laser pulses, for a large range of ambient

nitrogen pressures ranging from 10^{-6} Torr to 10^{2} Torr. Integrated emission intensity increases with pressure for both short-pulse and ultrafast excitations. Time of flight measurements have been carried out on the emission from neutral Ni I at 361.9 nm ($3d^9(^2D)\ 4p \rightarrow 3d^9(^2D)\ 4s$ transition), and ionic Ni II at 428.5 nm ($3p^6 3d^8(^3P)\ 4s \rightarrow 3p^6 3d^9\ 4s$), respectively. Measurements have been taken from two axial positions, viz. 2 mm and 4 mm away from the target surface, in the expanding plasma plume. A double-peak structure is observed in the TOF spectrum of Ni I under short-pulse excitation, in which the fast peak corresponds to neutrals formed by ion-electron recombination, and the slow peak corresponds to un-ionized neutrals ablated from the target. On the other hand, only a single fast peak is seen in the TOF spectrum of ultrafast excitation, the rising and falling edges of which correspond to recombined and un-ionized neutrals, respectively. Measured species velocities are relatively higher and independent of pressure for ultrafast excitation, whereas shockwave effects affect the velocity for short-pulse excitation. The velocities indicate that recombined neutrals and ions are clearly accelerating in the plume on expansion, at least up to a distance of 4 mm from the target, while the un-ionized neutrals get decelerated, particularly, at higher pressures. These studies provide important and new information on the temporal evolution of nickel plasmas produced by short-pulse and ultrafast laser pulses, which will be useful in applications including pulsed laser deposition and nanoparticle generation.

[1]C. Phipps, *Laser Ablation and its Applications* (Springer Science + Business media, LLC, 2007).
[2]S. R. Franklin and R. K. Thareja, Appl. Surf. Sci. **177**, 15 (2001).
[3]F. Garrelie, C. Champeaux, and A. Catherinot, Appl. Phys. A **69**, S55 (1999).
[4]D. B. Geohegan, Appl. Phys. Lett. **60**, 2732 (1992).
[5]P. E. Dyer and J. Sidhu, J. Appl. Phys. **64**, 4657 (1988).
[6]T. E. Itina, J. Hermann, P. Delaporte, and M. Sentis, Phys. Rev. E **66**, 066406 (2002).
[7]B. Rethfeld, K. Sokolowski-tinten, D. Von der Linde, and S. I. Anisimov, Appl. Phys. A **79**, 767 (2004).
[8]B. Verhoff, S. S. Harilal, J. R. Freeman, P. K. Diwakar, and A. Hussanein, J. Appl. Phys. **112**, 093303 (2012).
[9]A. Neogi, A. Mishra, and R. K. Thareja, J. Appl. Phys. **83**, 2831 (1998).
[10]S. S. Harilal, C. V. Bindhu, M. S. Tillack, F. Najmabadi, and A. C. Gaeris, J. Appl. Phys. **93**, 2380 (2003).
[11]S. Amoruso, R. Bruzzese, C. Pagano, and X. Wang, Appl. Phys. A **89**, 1017 (2007).
[12]S. Amoruso, G. Ausanio, R. Bruzzese, M. Vitiello, and X. Wang, Phys. Rev. B **71**, 033406 (2005).
[13]S. Amoruso, R. Bruzzese, X. Wang, N. N. Nedialkov, and P. A. Atanasov, J. Phys. D: Appl. Phys. **40**, 331 (2007).
[14]S. S. Harilal, N. Farid, A. Hassanein, and V. M. Kozhevin, J. Appl. Phys. **114**, 203302 (2013).
[15]See http://physics.nist.gov/PhysRefData/ASD/lines_form.html for standard NIST atomic spectral line database.
[16]S. S. Harilal, C. V. Bindhu, R. C. Issac, V. P. N. Nampoori, and C. P. G. Vallabhan, J. Appl. Phys. **82**, 2140 (1997).
[17]D. A. Cremers and L. J. Radziemski, *Handbook of Laser Induced Breakdown Spectroscopy* (John Wiley & Sons, Ltd., 2006).
[18]A. Couairon and A. Mysyrowics, Phys. Rep. **441**, 47 (2007).
[19]P. T. Rumsby and J. W. M. Paul, Plasma Phys. **16**, 247 (1974).
[20]N. Farid, S. S. Harilal, H. Ding, and A. Hassanein, J. Appl. Phys. **115**, 033107 (2014).
[21]J. J. Chang and B. E. Warner, Appl. Phys. Lett. **69**, 473 (1996).
[22]S. J. Henley, J. D. Carey, G. M. Fuge, M. N. R. Ashfold, and D. Anglos, Phys. Rev. B **72**, 205413 (2005).
[23]R. Sauerbrey, Phys. Plasmas **3**, 4712 (1996).
[24]J. A. Stamper, K. Papadopoulos, R. N. Sudan, S. O. Dean, E. A. McLean, and J. M. Dawson, Phys. Rev. Lett. **26**, 1012 (1971).
[25]J. R. Freeman, S. S. Harilal, P. K. Diwakar, B. Verhoff, and A. Hassanein, Spectrochim. Acta, Part B **87**, 43 (2013).
[26]N. Farid, S. S. Harilal, H. Ding, and A. Hassanein, Appl. Phys. Lett. **103**, 191112 (2013).